Shrink-Induced Microelectrode Arrays for Trace Mercury Ions Detection

Zonghao Wu and Tianhong Cui

***Abstract*— An ultrasensitive microelectrode arrays (MEA) mercury sensor based on the heat-shrinkable polymer was fabricated by a very simple and low-cost method for the first time. We sputter a comb-finger gold electrode on the heat-shrinkable polymer, made use of the heat shrinkage and sticky characteristics of the polymer to construct MEA, and then detected the trace mercury ions (Hg^{2+}) in the water by anodic stripping voltammetry. The characterization result indicated that the shrink polymer prepared by different heating temperature had controllable shrinkage ratios, and the electrode surface presented unique wrinkle structure by heating process. Due to the non-linear diffusion characteristic of the microelectrode and the microwrinkle structure, performance of the sensor had been improved greatly. The signal-to-noise ratio (Faraday current divide Background current) increased notably, and the sensor's detection limit was achieved as 0.0874 ppb. This is a very effective way to detect ultra-low concentrations mercury ions and the heat-shrinkable film-based microelectrode arrays construction method can be applied to many fields.**

***Index Terms*— Microelectrode arrays, shrink polymer, anodic stripping voltammetry, mercury sensor.**

I. Introduction

WATER pollution, especially heavy metal produces serious harm to human health because accumulated metals can enter an organism and lead to chronic poisoning [1], [2]. Mercury ions is the most concerned with water pollution that often exist at trace levels and coexist with a million-fold excess of other ionic species [3], [4]. Conventional instrumental detection methods for heavy metal ions in environmental samples include atomic absorption spectrometry (AAS), atomic fluorescence spectrometry (AFS), ion coupled plasma mass spectrometry (ICPMS), and microwave induced plasma atomic emission spectroscopy (MIP-AES) [5]–[7]. These methods require large-scale equipment, specialized laboratory rooms, and professional operating technicians. In the investigation of sudden environmental pollution incidents and ecological risk surveys at river basins and regional scales, due to the wide range of surveyed areas and the large number of environmental samples to be collected, high-throughput real-time field detection technologies are urgently needed [8]. Electrochemical detection technology provides feasible technical means for the portable equipment and rapid detection of trace level mercury ions in water samples.

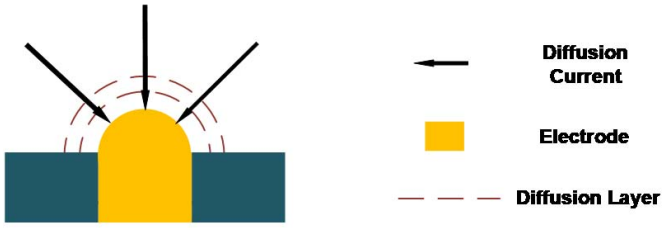

Fig. 1. Schematic diagram of nonlinear diffusion.

Anodic stripping voltammetry has many advantages such as high sensitivity, simplicity, minimal space and power requirements and low instrumentation cost [9], [10]. It has been successfully applied into environmental and waste water analysis for copper, cadmium, lead and chromium [11]–[13] etc. ASV method use the classic electrochemical electrode system and contains pre-concentration step and stripping step [14]. In order to achieve the best detection effect, more ions per unit time need to be accumulated in the pre-concentration step, which requires the electrode to have higher reaction intensity [15]. On the other hand, in the stripping step, the target ions on the surface of the electrode react to form a Faraday current(signal), and double-layer capacitance on the electrode surface charges and discharges to form a Non-Faraday current (background current), this is an important source of noise in the detection signal [16]. It is required that the sensor should have a high "signal-to-noise ratio", otherwise hard to detect low concentrations of heavy metal ions. Portable devices are generally fitted with micro sensors, due to its small size, ASV microsensor is generally difficult to achieve high detection performance [17]. So how to achieve high sensitivity and low detection limit detection performance on an ASV microsensor has been an important topic.

When the electrode size reduces to be equivalent to the thickness of the diffusion layer, diffusion current occurs along the electrode radius (rather than perpendicular to the electrode surface), called non-linear diffusion or radial diffusion (Fig.1). Compared to conventional electrochemical sensor, microelectrode arrays (MEA) sensor exhibits nonlinear diffusion with higher sensitivity, higher current density, faster mass transfer, and higher signal-to-noise ratio [18]–[20], these features are

Manuscript received August 5, 2018; revised November 18, 2018; accepted December 4, 2018. Date of publication December 21, 2018; date of current version March 7, 2019. The associate editor coordinating the review of this paper and approving it for publication was Dr. Chang-Soo Kim. *(Corresponding author: Tianhong Cui.)*

Z. Wu is with the Department of Precision Instrument, Tsinghua University, Beijing 100084, China (e-mail: wuzh14@mails.tsinghua.edu.cn).

T. Cui is with the Department of Electrical and Computer Engineering, University of Minnesota, Minneapolis, MN 55455 USA, and also with the Department of Biomedical Engineering, University of Minnesota, Minneapolis, MN 55455 USA (e-mail: cuixx006@umn.edu).

Digital Object Identifier 10.1109/JSEN.2018.2887269

very suitable as sensor for the ASV method. MEA sensor is widely applied for various ions sensing, shows good unique performance, but the fabrication process of MEA is always complex and high-cost, which limits the promotion and application of such sensors [21], [22]. The theory proves that the smaller the electrode size, the higher the signal-to-noise ratio at the microelectrode size [23].

When the heat-shrinkable film is heated over a certain temperature, the surface of the heat shrinkable film can be shrunk several times. This feature can be used for microelectrode processing to realize a smaller size electrode [24], [25]. Heat-shrinking a polymer substrate coated with metal thin film electrode can form wrinkle structure [26], [27], the micro/nano wrinkle structure can further enhance the nonlinear diffusion of the electrode surface. Moreover, fabrication of the shrink electrode is low-cost and does not require clean-room facilities or sophisticated equipment, this makes lower cost of sensors possible.

Herein, we reported an ultrasensitive microelectrode arrays mercury sensor based on heat-shrinkable polymer with a very simple and low-cost fabrication method. We constructed MEA though heating shrink polymer with comb-finger gold electrode and detected trace mercury ions in the water by anodic stripping voltammetry (ASV). Microelectrode arrays with unique wrinkle structure formed by heating-shrink could greatly facilitate the sensitive measurement of Hg (II). The performance of this microelectrode arrays based on new fabrication method for determination of Hg (II) was investigated in detail. Encouragingly, such a shrink polymer sensor offered a remarkably improved the signal-to-noise ratio and detection limit. The signal-to-noise ratio (Faraday current minus the background current) increased obviously, this is very conducive to the detection of ultra-low concentrations of mercury ions. This sensor‘s detection limit (LOD) of Hg (II) was achieved as 0.0874 ppb. This simple but effective high-performance sensor construction method can be widely used in the development of highly sensitive ion sensor.

II. Experimental

A. Chemicals and Reagents

Supporting electrolyte used was 0.1 M HCl buffer. Unless otherwise stated, deionized water (18.2 MΩ·cm) used throughout all experiments was prepared from a Milli-Q system (Millipore, Milford, MA, USA). All the pieces of glassware were thoroughly cleaned with aqua retia and then washed repeatedly with Millipore water and acetone before using. All the chemicals were purchased from Sigma-Aldrich unless mentioned specifically.

B. Apparatus

Shrink film (polyolefins, PS) was purchased from Sealed Air. An Ag/AgCl (3 M KCl) (Tianjin Aidahengsheng Technology Co., Ltd., China) was used as calibration reference electrode. A Gold electrode was used as counter electrode. Measurement were performed with CHI660e electrochemical (Chenhua Instruments Corporation, China) controlled by a personal computer.

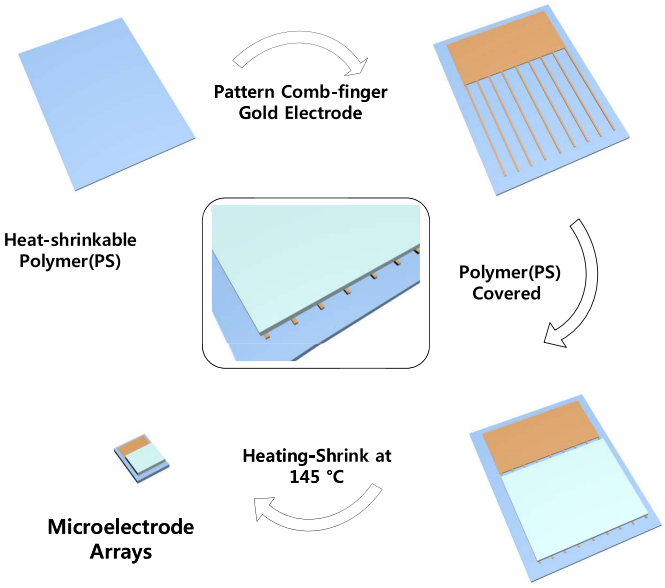

Fig. 2. Schematic diagram of an Hg (II) ultrasensitive sensor's fabrication process and structure diagram of the sensor.

C. Device Fabrication

Fig.2 illustrated the fabrication process and the schematic structure diagram of the sensor. First, a 30 nm gold film was patterned on a PS shrink film substrate by sputter process for the electrode. A comb-finger shape shadow mask was used to pattern the gold film. These fingers were designed with different widths (50μm, 100μm, 150μm) for our experimental discussion. Next, another heat-shrinkable film slightly smaller than the size of the substrate was covered the gold electrode surface. The position of this film determines the length of the electrode. Then, the sensor was heated to shrink at 145 °C, and the substrate and upper films was shrunk and stick together at the same time, and the front of electrodes with wrinkles structure surface form a characteristic microelectrode arrays.

D. Measurement Procedure

The optimized voltammetry conditions to determine Hg (II) in acetate buffer were as follows: Deposition potential (E_{dep}) = −0.2 V whilst stirring or vibrating for 100 s, with 20 s quiescence time and a voltammetric scan from 0 to 0.8 V. The scan mode used the square wave modulation, frequency 10 Hz, step height 4 mV, pulse height 20 mV.

III. Results and Discussion

A. Characterization

The optical image of broach gold electrode on a PS polymer substrate was shown in Fig.3a. Flexible PS film as a substrate sensor have a variety of application scenarios, and it is also adapted to roll-to-roll processing technology. As shown in Fig.3b, heating process completed the sensor‘s manufacture: the process significantly changed the size of the device and the surface area significantly reduced, at the same time the thickness increased. The comb-finger gold electrode became narrower and two layers of film was stuck together. The rear of the uncovered electrode could be connected with testing wire and the front formed microelectrode array.

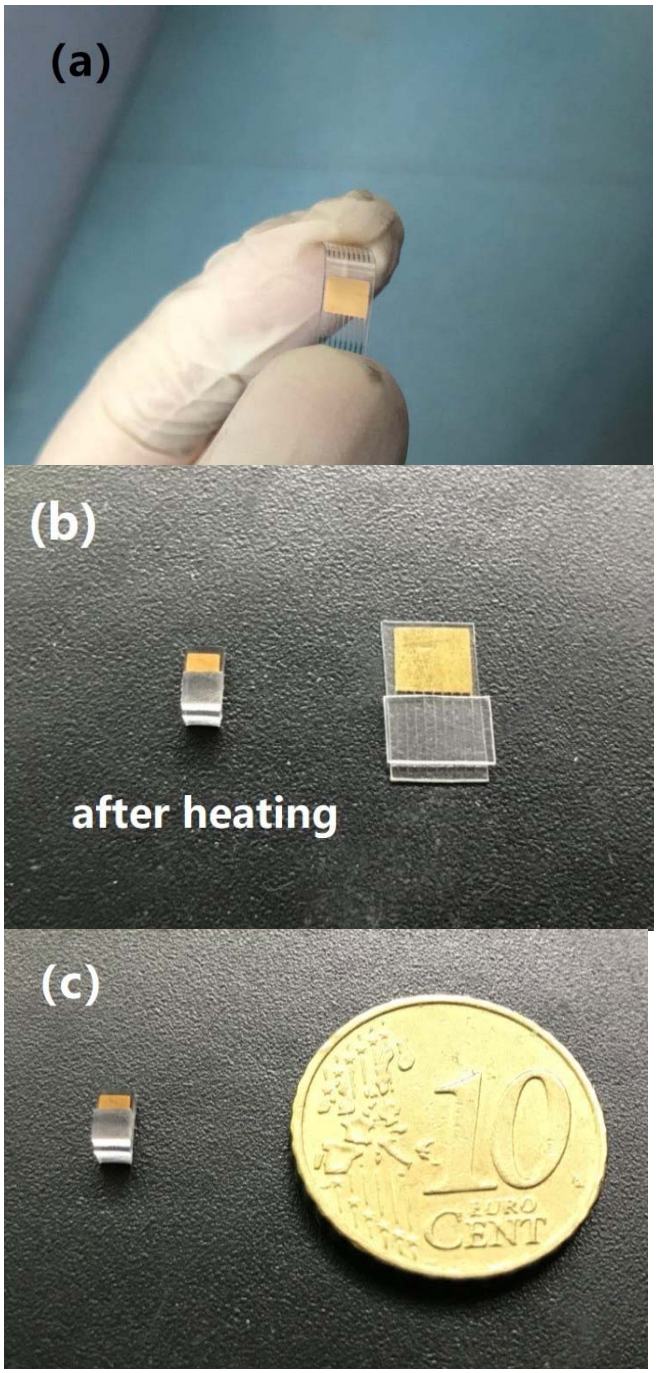

Fig. 3. (a) An optical image of the comb-finger gold electrode on PS substrate. (b) Heating process completed the sensor's manufacture. (c) An optical image of the MEA sensor based on heat-shrinkable polymer.

It was worth noting that all these micro electrodes had wrinkle surface, which is the unique structure that presented by heat-shrinking method. The optical image of the microelectrode arrays based on PS shrink polymer was shown in Fig.3c.

High temperature heating could shrink the PS polymer substrate because of the pre-stress effect:the surface area of the film significantly reduced, at the same time the thickness increased. To ensure the outcome, measurement of shrink ratio of a PS substrate was carried out. The PS substrate with width of 7 mm were prepared for this experiment and heated in an oven for 5 min with different temperature.

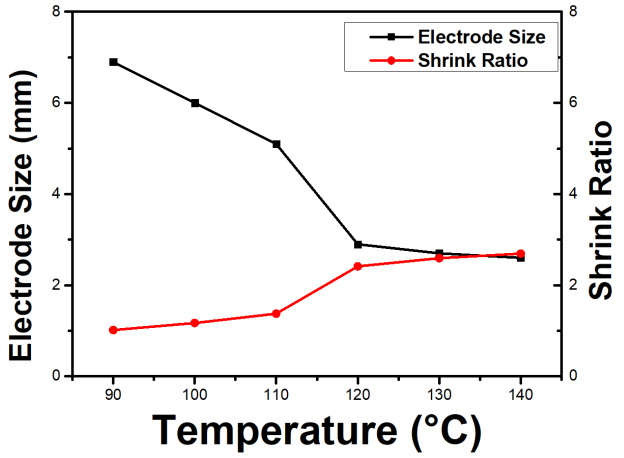

Fig. 4. The electrode size and shrink ratio of PS polymer substrate sensor with different temperature.

As shown in Fig. 4, when the temperature above 90 °C, PS polymer substrate starts to shrink evenly, the higher shrink temperature results in a higher contraction ratio. When the temperature achieved 140 °C, shrinkage of PS substrate reached its maximum, the temperature rise could not shrink the PS substrate further. Herein, the following equation was used for the shrink ratio calculation.

$$Shrink\ ratio = \frac{L_0}{L_T} \times 100\% \tag{1}$$

where L_0 is the initial area of the PS substrate and L_T is the area after heating at T °C. Sputtering and patterning the gold electrode on the PS substrate, when heated, because of the stress mismatch between the gold film and the PS substrate, the gold film appears fold and presents wrinkle structure. From the equation for shrink ratio, the rate of surface area of gold film, relative to the substrate, is quantitively calculated by the reciprocal of shrink ratio. As the heating temperature and the shrinkage ratio increase, wrinkle structure became more pronounced. Fig.5 shows the SEM images of the gold films on PS substrate and heating at 95 °C and 140 °C, respectively. As shown in Fig. 3, the maximum shrinkage ratio is about 2.7, it means that the 50μm width gold Electrode could shrink shaper to 18.5μm. This method could be used to break through the limit of micro-fabrication.

B. Effect of Microelectrode and Wrinkle Structure for Detection of Hg (II)

Mainly two reaction stages took place on the electrode surface of the sensor when using ASV method to detect mercury ion. In the first stage, a constant negative voltage was applied to the electrode, the mercury ion was reduced to single substance and adsorbed on the surface of the electrode, as in Equation 2. In this process, fixed stirring speed and deposition time were given, we could only though optimize the electrode material and surface morphology to accumulate more mercury. In the second stage, a positive scan voltage was applied to the electrode. Mercury was oxidized to mercury ions and dissolved in solution, as in Equation 3. This process produced the I-V output signal and the signal mainly included two parts, the Faraday current (Peak current, signal) produced by the

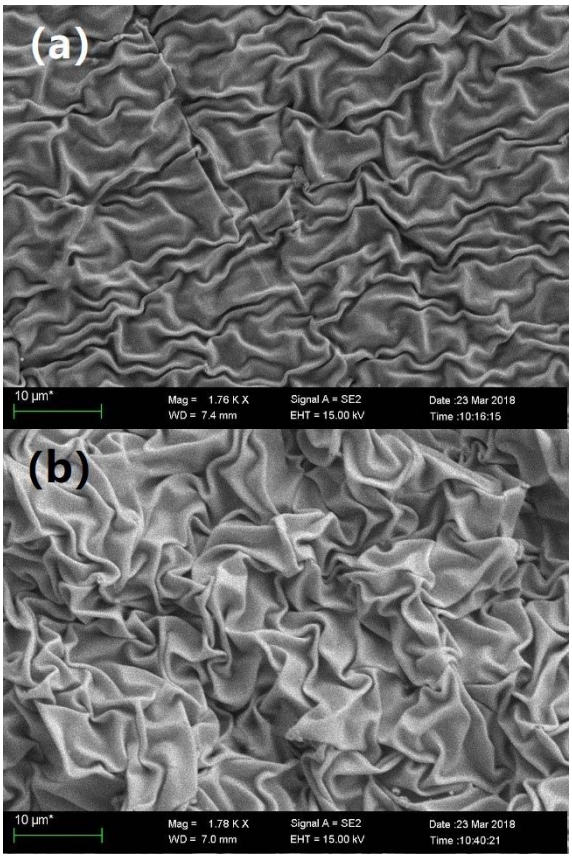

Fig. 5. (a) SEM image of gold film on a PS substrate heated at 95 °C. (b) SEM image of gold film on a PS substrate heated at 140 °C.

reaction of mercury, and Non-Faraday current (Background current, noise) generated by double layer capacitor (between the electrode and solution) charging and discharging. The high "signal-to-noise ratio" of the sensor facilitated the detection of low-level mercury ions. At this size of the microelectrode, the ratio had a direct relationship with the electrode radius, the smaller electrode radius, the higher "signal to noise ratio".

$$Hg^{2+} + 2e^{-} \rightarrow Hg \tag{2}$$

$$Hg \rightarrow Hg^{2+} + 2e^{-} \tag{3}$$

To evaluate the performance of heat-shrinking microelectrode arrays for very low concentrations of mercury ions, three kinds of sensors with PS substrate were fabricated and tested for our discussion. As shown in Fig.6a, the 1# sensor was a comb-finger (9 fingers) electrode with 50μm finger width and covered with tape on the top surface to form a microelectrode arrays structure. This sensor's fabrication process excluded heat shrinkage, so that gold film on the substrate had a flat surface relatively. The 2# sensors had 3 fingers (150 μm width) electrode and the 3# sensor had 9 fingers (50 μm width) electrode, they were both processed according to the schematic diagram of fabrication process shown in Fig.1. The three sensors were designed to have nearly the same surface area because of ASV sensor's surface area directy affected the magnitude of output signal.

The Cyclic Voltammetry(CV) measurement was performed using the $[Fe(CN)_6]^{3-/4-}$ redox couple to monitor the MEA sensor. As Shown in Fig.6b, the oxidation peak current and

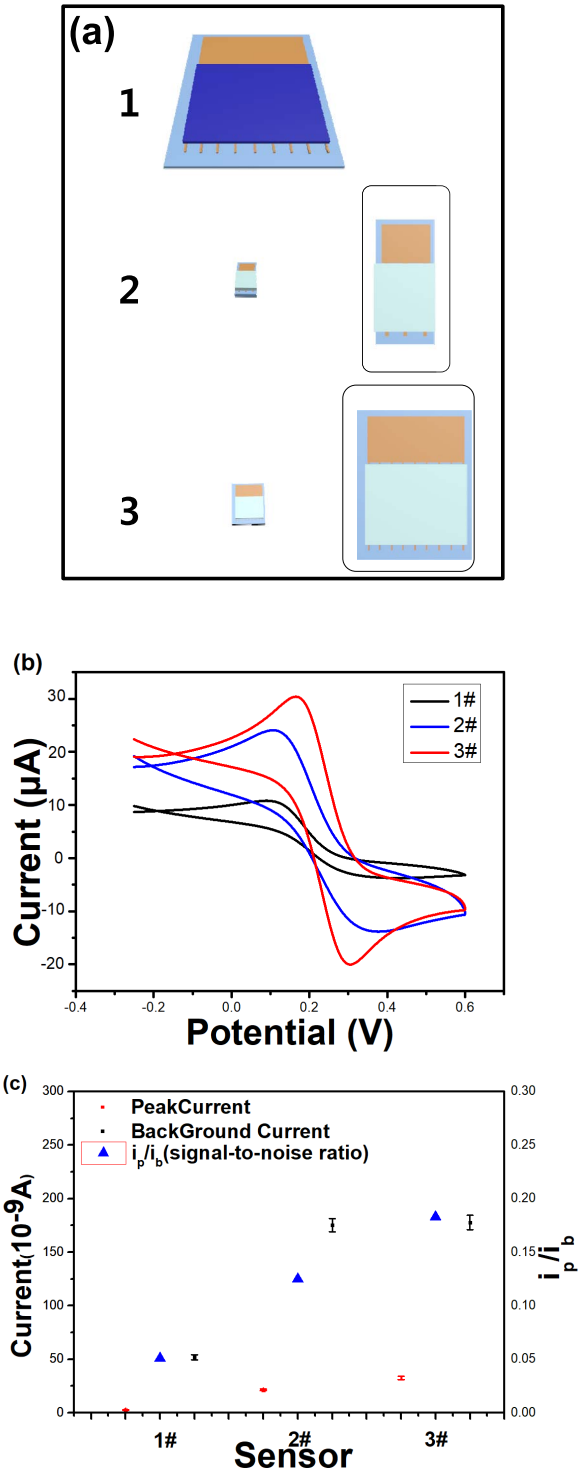

Fig. 6. (a) Three kinds of sensors with PS substrate were fabricated. (b) Cyclic voltammograms of three kinds of MEA sensors with 0.3 V/s scan rate in pH 7.5 PBS containing 5 mM $[Fe(CN)_6]^{3-/4-}$ and 0.1 M KCl. (c) Anodic Stripping Voltammetry results of 0.2 ppb Hg (II) solution measured by three kinds of MEA sensors.

the reduction peak current of these microelectrode sensors were almost equal, and the potential difference between the oxidation peak potential and the reduction peak potential was about 70 mV, which indicated the good electrochemical performance of these electrodes and the reaction on electrode surface had reversibility. This relatively simple electrode structure without a modified layer could exhibit controlled and

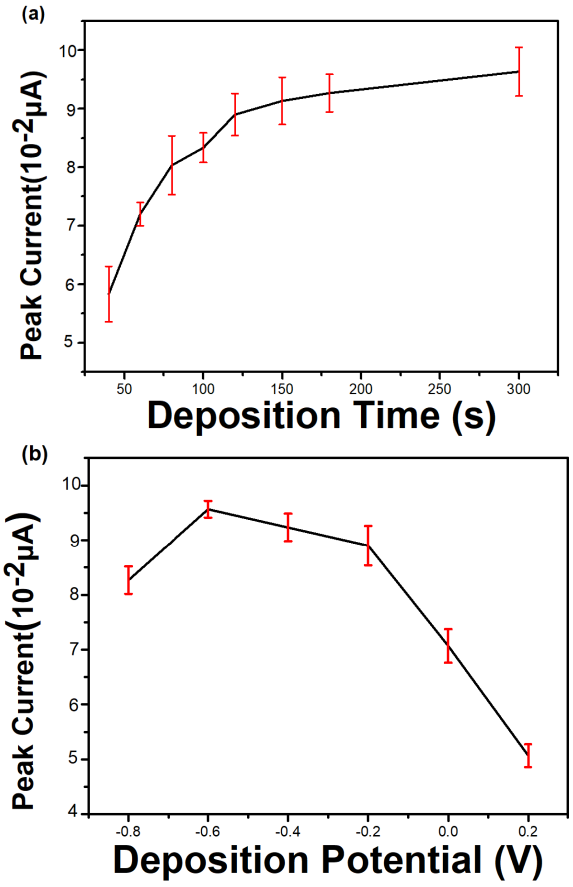

Fig. 7. Effect of the deposition time (a) and deposition potential (b) on the stripping peak current of 0.6 ppb Hg^{2+} solution on a 3# MEA sensor.

stable electrochemical performance, and it also had excellent detection capabilities. The 3# MEA sensor with smaller comb-finger electrode size and wrinkle structure got an obvious increase of peak current (curve 3#) compare to two other MEA sensors, caused by the nonlinear diffusion property of electrode surface which resulting in faster electron transfer and mass transfer rate.

Three kinds of MEA sensors were tested using ASV method in solution with 0.2 ppb Hg (II), respectively. As shown in Fig.6c, the peak current and background current of both 2# and 3# sensors were significantly higher than 1# sensor. It could be explained as the reaction on wrinkle structure surface was more dramatic and the mass transfer rate was higher. Comparing the testing results of the 2# and 3# electrodes, we could find that they had comparable background current, but the peak current of 3# electrode with a smaller finger width was larger, which also resulting in the "signal-to-noise ratio" improved for about 50%. The microelectrode arrays formed by the heat-shrinkage had good performance of detecting ultra-low concentration mercury ion solution due to its microelectrode effect and unique wrinkle structure.

C. ASV Determination of Hg (II)

The effect of the deposition time on the peak current of Hg^{2+} at -0.2 V deposition potential was studied in the time range from 40s to 300s and the obtained results are shown in Fig. 7a. All tests were given a 20s stop stirring time to obtain

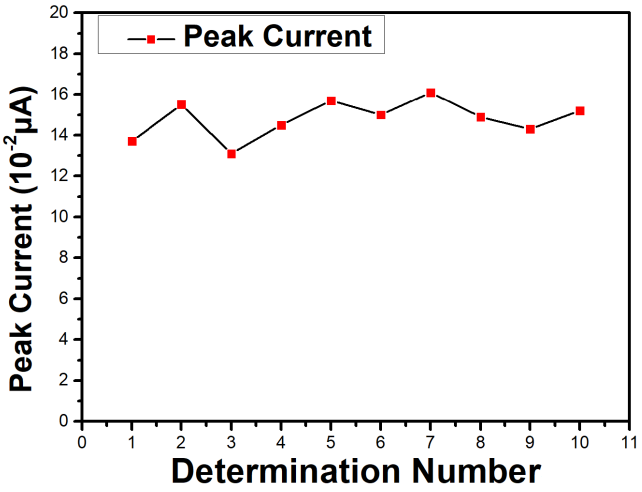

Fig. 8. Ten consecutive measurements for mercury solution with the concentration of 1.0 ppb using the same MEA sensor.

a static solution state. The stripping peak current of Hg^{2+} increased undoubtedly with the increase of the deposition time, because the surface of the electrode was covered by more mercury. Above 120s, the growth rate of peak current with the deposition time slowdown, which may be due to passivation of the electrode surface. Deposition time was chosen to be 120 seconds to balance limit of detection and measurement time. The effect of the deposition potential on the peak current of Hg^{2+} after 120s deposition time was also studied in the potential range from -0.8 V to 0.2s and the obtained results are shown in Fig. 7b. When the accumulation potential shifted from -0.2 V to -0.6 V, the stripping peak currents increased gradually. As the accumulation potential became more positive, the peak current reduced more completely. To a certain extent the more negative voltage can be beneficial to the accumulation of mercury ions. However, this trend was not the same at the deposition voltage of -0.8V. Because the reaction of water electrolysis was very violent at this voltage, a large number of bubbles appeared on the surface of the electrode, which was obviously not conducive to the enrichment of mercury ions, so that the peak discharge current was reduced. On the other hand, more negative voltages tended to concentrate other heavy metal ions such as Pb^{2+} and Cd^{2+} on the electrode surface, which might be detrimental to our detection. Therefore, -0.2 V was used as the optimal accumulation potential for the subsequent experiment.

The results of ten consecutive measurements for mercury solution with the concentration of 1.0 ppb using the same MEA sensor were shown in fig.8. Between each determination, multiple SWASV scanning without pre-concentration step was used to remove the deposited mercury of last test. The peak current fluctuated randomly at an average value of 0.147 μA and no upward or downward trend was observed. This indicated that our detection method was effective, and continuous detection did not lead to accumulation of mercury ions on the electrode surface and caused the unilateral increase of the stripping peak current. More importantly, this sensor was made of inert material gold as an electrode with a simple structure and did not have any modification layer. Therefore, it will not

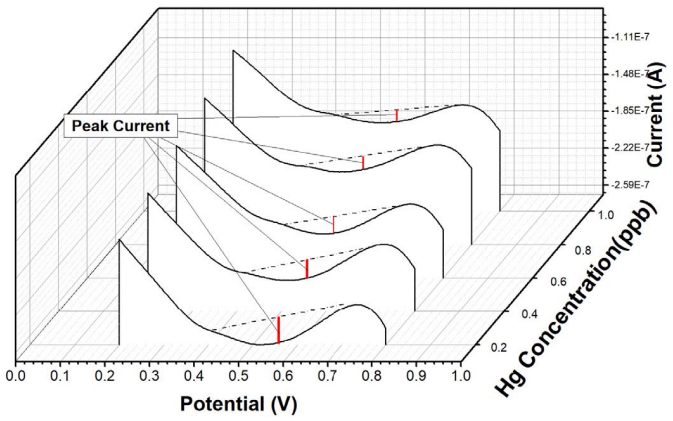

Fig. 9. Anodic stripping voltammograms of Hg (II) measured by the MEA sensor.

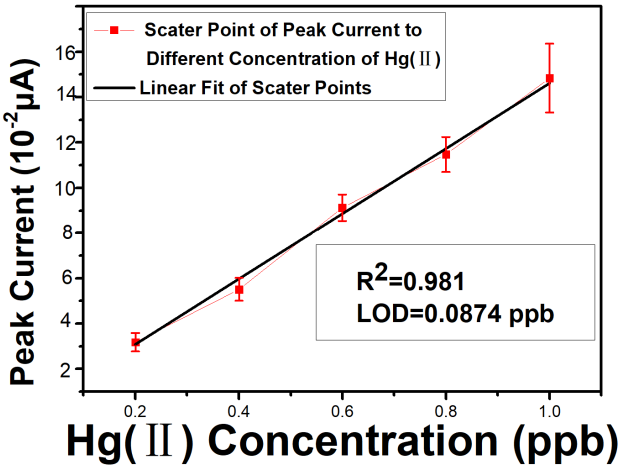

Fig. 10. Linear fitted calibration curve of Hg (II) from 0.2 to 1.0 ppb, with the limit of detection (LOD) derived as 0.0874 ppb.

cause significant performance degradation for multiple times applied. Compared to others that could only be used once due to the properties of the surface sensitive layer, or that need to be maintained manually, this MEA sensor had a huge cost advantage, which might expand more applications.

The MEA sensor's performance was characterized with 0.1 M HCl buffer solutions containing a series of concentrations of Hg^{2+}. We chose square wave anodic stripping voltammetry (SWASV) because this method can greatly reduce the background noise coming from the charging current during the stripping stage. Multiple SWASV scanning was used to remove the deposited mercury until the anodic stripping response disappeared. Meanwhile, the regeneration of the sensor surface was achieved.

Stripping voltammograms were obtained from 0.2 ppb to 1.0 ppb solutions with Hg (II) concentration increasing in 0.2 ppb steps, as shown in Fig.9. Corresponding calibration is shown in Fig.10, with 5 repeated measurements at each concentration. The detection limit is generally defined as three times the standard deviation of the noise. Sensitivity and limit of detection could be derived as 0.0874 ppb (S/N = 3) due to the high performance of LBL SA Graphene-Au NPs modification and heating-shrink process, respectively, according to the corresponding linear calibration plot, linearity coefficient of determination of 0.981 was achieved for the fitted plot.

IV. Conclusions

In summary, we present a very simple and low-cost microelectrode arrays fabrication method. Due to the non-linear diffusion characteristics of the micro-electrode and the micro-wrinkle structure formed by thermal shrinkage, the performance of the sensor has been greatly improved for mercury ions detection by ASV. The sensor's "signal-to-noise ratio" (Faraday current divide background current) increases significantly, and detection limit is achieved as 0.0874ppb. Testing results show that this is an effective means to detect ultra-low concentrations of mercury ions. In addition, this processing idea may be applied to various fields.

Acknowledgments

The authors greatly appreciate help from Hongyan Yu for the fabrication of micro gold electrode.

References

[1] M. Bader, M. C. Dietz, A. Ihrig, and G. Triebig, "Biomonitoring of manganese in blood, urine and axillary hair following low-dose exposure during the manufacture of dry cell batteries," *Int. Arch. Occupat. Environ. Health*, vol. 72, no. 8, pp. 521–527, 1999.

[2] P. Zhuang, M. B. McBride, H. Xia, N. Li, and Z. Li, "Health risk from heavy metals via consumption of food crops in the vicinity of Dabaoshan mine, South China," *Sci. Total Environ.*, vol. 407, no. 5, pp. 1551–1561, 2009.

[3] F. Zahir, S. R. Rizwi, S. K. Haq, and R. H. Khan, "Low dose mercury toxicity and human health," *Environ. Toxicol. Pharmacol.*, vol. 20, no. 2, pp. 351–360, 2005.

[4] A. T. Townsend, K. A. Miller, S. McLean, and S. Aldous, "The determination of copper, zinc, cadmium and lead in urine by high resolution ICP-MS," *J. Anal. At. Spectrometry*, vol. 13, no. 11, pp. 1213–1219, 1998.

[5] J. L. Gómez-Ariza, F. Lorenzo, and T. García-Barrera, "Comparative study of atomic fluorescence spectroscopy and inductively coupled plasma mass spectrometry for mercury and arsenic multispeciation," *Anal. Bioanal. Chem.*, vol. 382, no. 2, pp. 485–492, 2005.

[6] C. F. Harrington, S. A. Merson, and T. M. D'Silva, "Method to reduce the memory effect of mercury in the analysis of fish tissue using inductively coupled plasma mass spectrometry," *Analytica Chim. Acta*, vol. 505, no. 2, pp. 247–254, 2004.

[7] M. A. Nolan and S. P. Kounaves, "Microfabricated array of iridium microdisks as a substrate for direct determination of Cu^{2+} or Hg^{2+} using square-wave anodic stripping voltammetry," *Anal. Chem.*, vol. 71, no. 16, pp. 3567–3573, 1999.

[8] C. Kokkinos, A. Economou, I. Raptis, and T. Speliotis, "Disposable microfabricated bismuth microelectrode arrays for trace metal analysis by stripping voltammetry," *Procedia Eng.*, vol. 25, no. 35, pp. 880–883, 2011.

[9] S.-H. Shin and H.-G. Hong, "Anodic stripping voltammetric detection of arsenic (III) at platinum-iron (III) nanoparticle modified carbon nanotube on glassy carbon electrode," *Bull. Korean Chem. Soc.*, vol. 31, no. 11, pp. 3077–3083, 2010.

[10] C. Kokkinos, A. Economou, I. Raptis, and T. Speliotis, "Novel disposable microfabricated antimony-film electrodes for adsorptive stripping analysis of trace Ni(II)," *Electrochem. Commun.*, vol. 11, no. 2, pp. 250–253, 2009.

[11] J. Liu, J. B. Mahony, and P. R. Selvaganapathy, "Low-cost and versatile integration of microwire electrodes and optical waveguides into silicone elastomeric devices using modified xurographic methods," *Microsyst. Nanoeng.*, vol. 3, p. 17040, Oct. 2017.

[12] O. Abollino, A. Giacomino, M. Malandrino, G. Piscionieri, and E. Mentasti, "Determination of mercury by anodic stripping voltammetry with a gold nanoparticle-modified glassy carbon electrode," *Electroanalysis*, vol. 20, no. 1, pp. 75–83, 2008.

[13] J. Tu, H. Wan, and P. Wang, *Micro/Nano Electrochemical Sensors for Ion Sensing*. Singapore: Springer, 2016.
[14] Z. Wu, G. Jing, and T. Cui, "An ultrasensitive mercury sensor based on self-assembled graphene and gold nanoparticles on shrink polymer," in *Proc. 19th Int. Conf. Solid-State Sensors, Actuat. Microsyst.*, 2017, pp. 234–237.
[15] M. Sarajlić, Z. Đurić, V. Jović, S. Petrović, and D. Đorđević "Detection limit for an adsorption-based mercury sensor," *Microelectron. Eng.*, vol. 103, pp. 118–122, Mar. 2013.
[16] C. G. Chen, J. Zhang, Y. Du, X. Yang, and E. Wang, "Microfabricated on-chip integrated Au–Ag–Au three-electrode system for in situ mercury ion determination," *Analyst*, vol. 135, no. 5, pp. 1010–1014, 2010.
[17] Z. Bi, C. S. Chapman, P. Salaün, and C. M. G. van den Berg, "Determination of lead and cadmium in sea-and freshwater by anodic stripping voltammetry with a vibrating bismuth electrode," *Electroanalysis*, vol. 22, no. 24, pp. 2897–2907, 2010.
[18] Z. Guo, F. Feng, Y. Hou, and N. Jaffrezic-Renault, "Quantitative determination of zinc in milkvetch by anodic stripping voltammetry with bismuth film electrodes," *Talanta*, vol. 65, no. 4, pp. 1052–1055, 2005.
[19] N. Lezi, A. Economou, P. A. Dimovasilis, P. N. Trikalitis, and M. I. Prodromidis, "Disposable screen-printed sensors modified with bismuth precursor compounds for the rapid voltammetric screening of trace Pb(II) and Cd(II)," *Analytica Chim. Acta*, vol. 728, no. 22, pp. 1–8, 2012.
[20] R. G. Compton, G. G. Wildgoose, N. V. Rees, I. Streeter, and R. Baron, "Design, fabrication, characterisation and application of nanoelectrode arrays," *Chem. Phys. Lett.*, vol. 459, nos. 1–6, pp. 1–17, 2008.
[21] D. W. M. Arrigan, "Nanoelectrodes, nanoelectrode arrays and their applications," *Analyst*, vol. 129, no. 12, pp. 1157–1165, 2004.
[22] M. O. Salles, A. P. R. de Souza, J. Naozuka, P. V. de Oliveira, and M. Bertotti, "Bismuth modified gold microelectrode for Pb(II) determination in wine using alkaline medium," *Electroanalysis*, vol. 21, no. 12, pp. 1439–1442, 2009.
[23] S. Zhang *et al.*, "Real-time simultaneous recording of electrophysiological activities and dopamine overflow in the deep brain nuclei of a non-human primate with Parkinson's disease using nano-based microelectrode arrays," *Microsyst. Nanoeng.*, vol. 4, p. 17070, Jan. 2018.
[24] A. Hauke *et al.*, "Superwetting and aptamer functionalized shrink-induced high surface area electrochemical sensors," *Biosensors Bioelectron.*, vol. 94, pp. 438–442, Aug. 2017.
[25] M. C. Wang, S. Chun, R. S. Han, A. Ashraf, P. Kang, and S. Nam, "Heterogeneous, three-dimensional texturing of graphene," *Nano Lett.*, vol. 15, no. 3, pp. 1829–1835, 2015.
[26] B. Zhang, M. Zhang, K. Song, Q. Li, and T. Cuia, "Shrink induced nanostructures for energy conversion efficiency enhancement in photovoltaic devices," *Appl. Phys. Lett.*, vol. 103, no. 2, pp. 133–135, 2013.
[27] J. D. Pegan, A. Y. Ho, M. Bachman, and M. Khine, "Flexible shrink-induced high surface area electrodes for electrochemiluminescent sensing," *Lab A Chip*, vol. 13, no. 21, pp. 4205–4209, 2013.

Zonghao Wu received the B.S. degree from the School of Automation Engineering, University of Electronic Science and Technology of China, Chengdu, China, in 2011. He is currently pursuing the Ph.D. degree with the Department of Precision Instrument, Tsinghua University, Beijing, China. His research interests include MEMS chemical sensors, embedded computing and controlling systems, and the Internet of Things.

Tianhong Cui is currently a Distinguished McKnight University Professor with the University of Minnesota. He is also a Professor of Mechanical Engineering and an Affiliate Senior Member of the Graduate Faculty with the Department of Electrical Engineering and the Department of Biomedical Engineering. He is also an Adjunct Professor with Mayo Clinic and a Distinguished Visiting Professor with the University of Paris-Est, France. He has over 310 archived publications in scientific journals and prestigious conferences. His current research interests include MEMS and nanotechnology. He is a Fellow of the American Society of Mechanical Engineering. He is a Distinguished Visiting Fellow at the Royal Academy of Engineering, U.K. He is the Founding Executive Editor-in-Chief of *Microsystems Nanoengineering*. He is also serving as the Founding Editor-in-Chief for the first AAAS/Science Partner Journal *Research*.